

David A. Rupp\*  
Lee F. Mortimer  
Michael Fairweather

# Improvements to Stochastic Approaches for Simulating Agglomeration in Particle-Laden Flows

Direct numerical simulation, facilitated by the spectral element method, has been used to study collisions and agglomeration in particle-laden fluid flows through a channel at shear Reynolds number. The particulate phase is simulated by deterministic Lagrangian particle tracking alongside a stochastic technique to resolve collisions. Interestingly, the implementation of agglomeration in the deterministic approach caused a major reduction in the particle collision rate. To determine the cause of this effect, analysis of the collision rate and location across the channel for different particle properties was performed. For systems without agglomeration, collisions between particles tend to be located on consistent streamlines, occurring between single pairs of particles. A numerical analysis of this effect confirmed the result, where inter-particle collisions across the channel mostly took place between consistent particle pairs in close proximity. Repeat collisions are shown to be almost eliminated with the addition of the agglomeration mechanism. The impact and implications of this effect on the accuracy of the stochastic technique is discussed, and modifications are suggested to offer improvements while accounting for the repeat collisions.

 This is an open access article under the terms of the Creative Commons Attribution-NonCommercial License, which permits use, distribution and reproduction in any medium, provided the original work is properly cited and is not used for commercial purposes.

**Keywords:** Agglomeration, Direct numerical simulation, Lagrangian particle tracking, Particle collisions, Stochastic method

*Received:* December 13, 2022; *revised:* February 23, 2023; *accepted:* April 17, 2023

**DOI:** 10.1002/ceat.202200597

## 1 Introduction

Accurate simulation of particle-laden flows is of fundamental importance to any area of industry that will at some point be required to transport a fluid-solid multiphase component of its process or waste to a new location. Multiphase flow simulations are frequently performed in industries which refine and transport chemicals, such as agriculture [1], pharmaceuticals [2], and minerals processing [3]. The core electrical energy generation methods, based on coal, oil, and gas, are also obvious examples that handle multiphase flows [4]. Without informed optimization, industrial processes can be inefficient, unsafe, and costly, due to the amount of maintenance required, or the need for part replacement, which can often be hazardous. This is particularly true of nuclear waste processing where exposure to radioactive or otherwise dangerous materials is possible.

The dynamic properties and complex mechanisms of turbulent wall-bounded flows demand high levels of mathematical accuracy for the purpose of making predictions of their chaotic behavior. A minute change in system parameters and initial conditions will often inextricably lead to differing instantaneous results over long timescales. In the case of experimental studies, this sensitivity to initial conditions can lead to unreliable reproducibility, for said conditions are tremendously diffi-

cult to isolate, more so as the Reynolds number increases. For a more accessible representation of the flow, computational methods such as large eddy simulation (LES) and direct numerical simulation (DNS) are available. Both methods involve constructing a numerical mesh for resolving small-scale effects with high accuracy, and then further solving the Navier-Stokes equations at relevant scales.

Traditionally, the Lagrangian particle tracking (LPT) method has been used to simulate the movement of particles and the collisions thereof. In this case, particles are modeled as point spheres and an integrated force-balance equation of motion is used to calculate advection on them. This method, whilst accurate, suffers from similar computational constraints to DNS, where collision calculations become unfeasible for large particle numbers, often required for the representation of industrial flows.

---

Dr. David A. Rupp (pmdr@leeds.ac.uk), Dr. Lee F. Mortimer, Prof. Michael Fairweather  
School of Chemical and Process Engineering, Faculty of Engineering and Physical Sciences, University of Leeds, Leeds, LS2 9JT, United Kingdom.

In spite of these drawbacks, LPT has been used to great success in modeling multiphase turbulent flows, particularly in channels, with significant progress made in understanding turbophoresis, the process by which particles are moved towards the walls [5] through the influence of turbulence. For instance, recent findings show that the consideration of particles leads to an increase in the bulk flow rate and turbulent length scales for certain cases, and that the interparticle collisions cause a reduction in the near wall accumulation caused by turbophoresis [6].

One alternative to the Lagrangian method of colliding particles is the stochastic method [7], for which computational complexity scales with the number of particles, rather than the number squared. The method calculates the likelihood of a particular particle colliding through the generation of a fictitious collision partner, which is representative of the local particle phase properties, so that no information is required on the actual position and direction of motion of the surrounding real particles [7]. This then resolves the correct number of collisions for the flow based on a collision probability and the averaged statistics of the particles in the same region.

This study investigates this methodology in conjunction with a channel flow geometry where both inter-particle collisions and agglomeration are considered. It assesses an unexpected condition that the implementation of agglomeration causes with the stochastic method, namely, an excessively high collision rate, and determines a cause and potential solution.

## 2 Methodology

To simulate the continuous phase, a spectral element method (SEM) is used to determine the action of the fluid. The SEM is a hybrid of the finite element and the spectral methods. Combining the accuracy of the spectral method with the generality of the finite element method leads to a much more flexible technique for solving the incompressible Navier-Stokes equations. The code employed, Nek5000 [8], has been extensively tested and validated, and contains efficient parallelization capabilities as well as the flexibility to include an effective particle phase model.

The SEM is implemented by dividing the fluid domain into smaller elements, the number and shape of which are determined by the geometry of the domain and by the intended resolution of the program, with enough flexibility to accommodate common and indeed uncommon fluid domains. This work used DNS, so the element spacings used have an upper bound for size, which is ideally no greater than 15 times the Kolmogorov length scale [9]. The non-dimensionalized Navier-Stokes equations can be stated as:

$$\frac{d\mathbf{u}^*}{dt^*} + (\mathbf{u}^* \nabla) \mathbf{u}^* = -\nabla p^* + \frac{1}{Re_B} \nabla \tau^* + f_i \quad (1)$$

$$\nabla \cdot \mathbf{u}^* = 0 \quad (2)$$

Here,  $\mathbf{u}^*$  is the fluid velocity vector, which has been non-dimensionalised in terms of the bulk velocity  $U_B$ , and  $t^*$  is an expression of non-dimensionalised time,  $t^* = tU_B/\delta$ , where  $\delta$  is the channel half height. The term  $p^*$  is a non-dimensionalized

pressure term,  $p^* = p/\rho_F U_B^2$ , where  $\rho_F$  is the density of the continuous phase.  $Re_B$  is the bulk Reynolds number given by  $Re_B = \delta U_B/\nu$ , and  $\tau^*$  is the non-dimensionalised deviatoric stress tensor,  $\tau^* = (\nabla \mathbf{u}^* + \nabla \mathbf{u}^{*T})$ . The final term,  $f_i$ , represents body forces on cell  $i$ , given by  $\mathbf{f}_i = \mathbf{f}_{PG} + \mathbf{f}_{2W}^i$ . The flow is driven by a constant pressure gradient term  $\mathbf{f}_{PG} = (Re_\tau/Re_B)^2 \mathbf{x}^*$ , with  $\mathbf{x}^*$  a unit vector in the streamwise direction. The term  $\mathbf{f}_{2W}^i$  represents two-way momentum exchange between the fluid and particulate phases, detailed later.

These equations were solved by Nek5000 for an initially turbulent fluid flow in a channel geometry of  $12 \times 2 \times 6$  non-dimensional distance units where the  $12(x^*)$  and  $6(z^*)$  dimensions enforced continuous, periodic boundaries, and the  $2(y^*)$  dimension was wall-bounded with a no-slip condition at either extent. At  $Re_\tau = 300$  this was simulated using a  $32 \times 32 \times 32$  element mesh with spectral discretization order  $N = 7$ , i.e., a total of 11.2M equivalent cells.

In order to model the dispersed particle phase of a multiphase flow, a Lagrangian particle tracker was first employed which was developed in conjunction with the Nek5000 code used in this study. The Lagrangian particle tracking routine tracks individual particles as computational spheres, and time-evolves their velocity and position synchronously with the Eulerian fluid flow model, operating over the same time steps and representing the fluid-particle interactions by solving the non-dimensional equations of motion described below:

$$\frac{\partial \mathbf{x}_p^*}{\partial t^*} = \mathbf{u}_p^* \quad (3)$$

$$\frac{\partial \mathbf{u}_p^*}{\partial t^*} = \frac{1}{M_{VM}} \times \left[ \underbrace{\frac{3C_D |\mathbf{u}_s^*|}{4d_p^* \rho_p^*} \mathbf{u}_s^*}_{\text{Drag}} + \underbrace{\frac{3}{4} \frac{C_L}{\rho_p^*} (\mathbf{u}_s^* \times \omega_F^*)}_{\text{Lift}} + \underbrace{\frac{1}{2\rho_p^*} \frac{D\mathbf{u}_F^*}{Dt^*}}_{\text{Virtual mass}} + \underbrace{\frac{1}{\rho_p^*} \frac{D\mathbf{u}_F^*}{Dt^*}}_{\text{Pressure gradient}} \right] \quad (4)$$

$$M_{VM} = \left( 1 + \frac{1}{2\rho_p^*} \right) \quad (5)$$

The fourth-order Runge-Kutta method, also known as RK4 [10], was used to solve these equations for each particle within every time step in the Lagrangian particle tracker. Here,  $d_p^*$  and  $\rho_p^*$  are, respectively, the non-dimensional diameter and density ratio of the particle, and  $\mathbf{u}_s^*$ ,  $\mathbf{u}_F^*$ , and  $\omega_F^*$  are the non-dimensional slip velocity, fluid velocity, and vorticity, with  $C_D$  and  $C_L$  being the coefficients of drag and lift. The virtual mass term,  $M_{VM}$  is substituted into the equation.

For increased volume fraction flows where collision effects are dominant, the impact of the particles on the fluid must be considered. The two-way coupling momentum exchange term is included in the final term of Eq. (1) to account for this:

$$\mathbf{f}_{2W}^i = \frac{1}{V_i} \sum_j \frac{\partial \mathbf{u}_{pj}^*}{\partial t^*} \quad (6)$$

where  $V_i^*$  is the volume of a computational cell, and  $j$  loops over each particle contained within in that cell.

The deterministic particle interactions, obtained based on the LPT, were treated as hard sphere collisions, with collision times smaller than the LPT time step, and additional interparticle forces were either ignored as negligible or partially implemented as part of the agglomeration mechanism. To reduce computational demand, the domain was reduced into smaller cells, with only particles in the same cell considered as potential collision partners. The non-dimensional radii of the particles considered in this study were  $r_p^* = 0.005$  and  $0.01$ , equivalent to  $100\mu\text{m}$  and  $200\mu\text{m}$  particles in a channel with  $\delta = 0.02\text{m}$  with shear Stokes numbers in water of  $0.31$  and  $1.25$ , respectively.

A deterministic energy-balance method was used to calculate the energetic collision conditions under which a particle agglomerate forms, as employed by Njobuenwu and Fairweather [11]. This is given as:

$$\mathbf{u}_{p,\text{rel}}^{*2} - \frac{(1 - e_n^{*2}) (\mathbf{u}_{p,\text{rel}}^* \hat{\mathbf{n}})^2}{|\mathbf{u}_{p,\text{rel}}^* \hat{\mathbf{n}}|} \leq \frac{H^*}{6\delta_0^{*2}} \left[ \frac{6(1 - e_n^{*2})}{\pi^2 \rho_p \sigma^*} \left( \frac{d_{p,i}^{*3} + d_{p,j}^{*3}}{d_{p,i}^{*2} d_{p,j}^{*2} (d_{p,i}^* + d_{p,j}^*)} \right) \right]^{1/2} \quad (7)$$

where  $H^*$  is the non-dimensional Hamaker constant, given by  $H^* = H/\rho_F U_B^2 \delta^3$ ,  $\delta_0^* = \delta_0/\delta$  is the non-dimensional minimum contact distance and  $\hat{\mathbf{n}}$  is a unit vector pointing between the colliding particle pair, and  $\mathbf{u}_{p,\text{rel}}^{*2}$  is the relative velocity between the colliding particles;  $e_n^*$  is the normal coefficient of restitution. The coefficient of restitution is set to  $0.4$  for all simulations studied in this work to match collisions between particles made of calcite, a typical simulant for nuclear waste material in nuclear waste transport flows where predicting aggregation is of importance from an economic and safety point of view.

The scope of this study is restricted to only one coefficient of restitution, although the repeat collision effect is expected to exist as the coefficient approaches the elastic ratio. Upon collision, if the condition stated in the equation is satisfied, the particles are considered to combine into a spherical agglomerate with radius calculated such that the new volume is equivalent to the summed volume of its constituents.

Rupp et al. [12] introduced a modified stochastic technique for use in channel flows, which employs advective theory as derived by Saffman and Turner [13] using a direct simulation Monte Carlo (DSMC) technique similarly to Pawar et al. [14]. This calculates the particle collision rate within a given strata of a flow, a cell encompassing the entirety of the channel in the streamwise and spanwise dimensions, and a small section in the wall-normal dimension, matching the fluid elements used. The probability of collision for a particle is given as:

$$P_{\text{coll}} = \left( \frac{8\pi}{15} \right)^{1/2} n_p (d_p)^3 \left( \frac{\varepsilon}{\nu} \right)^{1/2} \Delta t \quad (8)$$

where  $\varepsilon$  is the turbulence kinetic energy dissipation rate,  $\nu$  is the kinematic viscosity, and  $n_p$  and  $d_p$  are the particle number

density and the diameter, respectively. Two classes of particle were simulated using both the deterministic and stochastic techniques. Further simulations were performed for both cases with the agglomeration mechanism active.

As will be made apparent in the discussion section, improvements were required to be made to the code where the stochastic technique was employed in a model with agglomeration. These modifications were based on observations made by Wang et al. [15], where the below equation relates to the modification of the collision rate due to certain interparticle effects such as the accumulation effect, i.e., where small-scale dissipative turbulent eddies enhance the particle collision rate by inducing a non-uniform local particle distribution:

$$\frac{\Gamma}{\Gamma_0} = 4.85 \frac{\eta}{r} g(r) \frac{|w_r|}{u_\eta} \quad (9)$$

Here,  $\eta$  and  $u_\eta$  represent, respectively, the Kolmogorov length and velocity scales,  $r$  is the particle radius, and  $g(r)$  is a statistical function of the radius known as the radial distribution at contact which directly measures the accumulation effect;  $|w_r|$  represents the Lagrangian pair relative velocity statistics of particles and is a measure of the turbulent transport effect.

### 3 Results and Discussion

The baseline case for this study was a four-way coupled deterministic simulation of a turbulent channel flow without agglomeration, i.e., both particle-fluid and particle-particle interactions were taken into account. This was performed for particles with varying radii,  $r_p^* = 0.005$  and  $0.01$ , and particle numbers,  $300k$  and  $2.2M$ . The results of these simulations were previously compared with the outcomes using the DSMC stochastic technique, showing good agreement [12].

The results of the deterministic simulations are illustrated in Fig. 1. Additional simulations using the agglomeration mechanism generated useful results surrounding both the impact of particles on the fluid as well as the rate of particulate aggregation in a simple wall-bounded flows. In general, the effect of agglomeration on the mean fluid streamwise velocities and the normal and shear stresses was small over the simulation time considered.

Of the cases considered, the system with the most significant change was the channel populated with the higher radius  $r_p^* = 0.01$  particles, with results shown in Fig. 1c. The inclusion of high Stokes number particles can be seen to have affected the overall particle statistics slightly, and the fluid statistics less so (with little difference visible between the lines with and without agglomeration). Previous studies by the authors in this geometry and Reynolds number have shown the mean streamwise velocity to be resistant to change, and likewise here the streamwise particle velocity displayed in Fig. 1 is seen to be minimally impeded towards the center of the channel.

The normal and shear stresses for the same conditions are likewise minimally affected. The largest change seen is in the spanwise fluid velocity fluctuations within the bulk flow at  $0.3 < y^* < 0.7$ , a region shown in previous studies to be particularly affected by changes in the particle Stokes number [16].

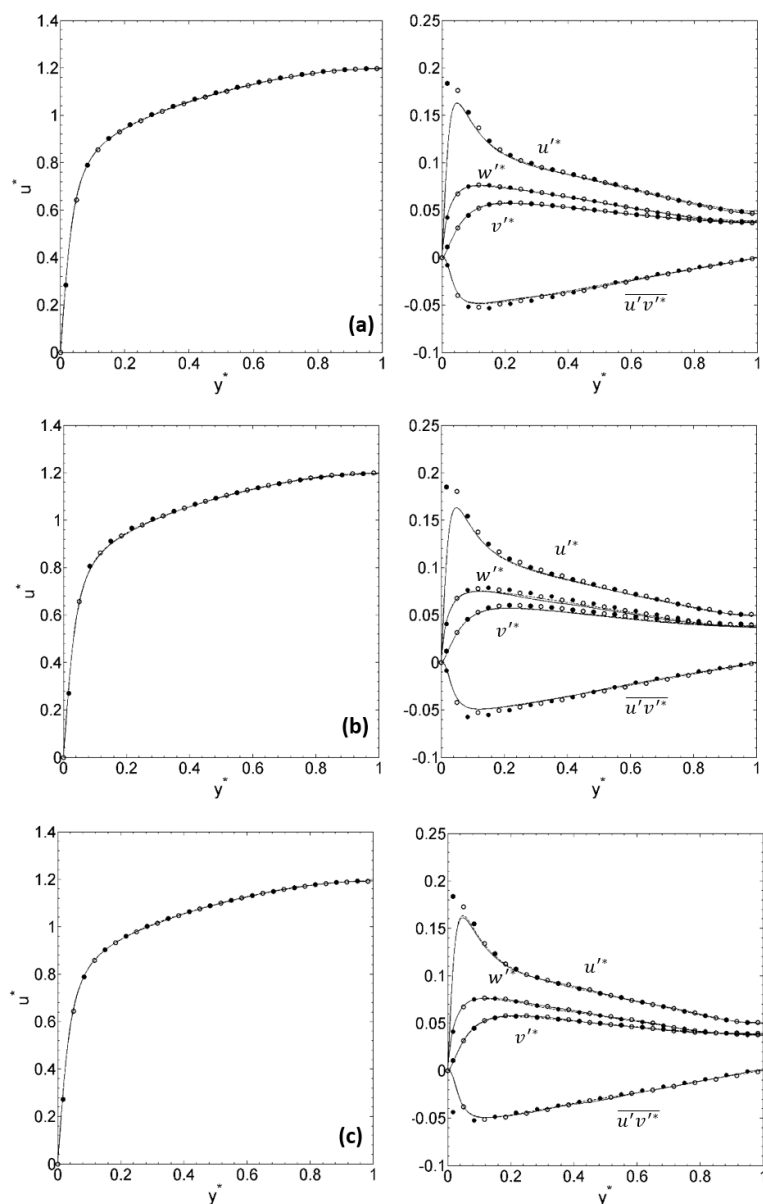


**Figure 1.** Mean streamwise velocities  $u^*$  and normal and shear stresses  $u'^2$ ,  $v'^2$ ,  $w'^2$ ,  $u'v'^2$  for fluid flows with particles collided with and without agglomeration. Fluid simulated — with and - - - without agglomeration, and particles ● with and ○ without agglomeration. For simulations with (a) 300k, 100µm ( $r_p^* = 0.005$ ), (b) 300k, 200µm ( $r_p^* = 0.01$ ), and (c) 2.2M, 100µm particles.

The evolution of agglomerates over time for these cases was also analyzed and this can be seen later below.

Having demonstrated the DSMC stochastic technique for the prediction of collisions in previous work, the model was

incorporated into the overall model which employed the additional post-collision agglomeration mechanism. However, this resulted in an immediate upturn in agglomeration when compared to the deterministic interaction flow, to the point where the simulations could not handle the effects on the fluid flow from the sudden appearance of many high Stokes number particles created by agglomeration. This made it clear that there were other factors that needed consideration in order for the stochastic technique to be effective where agglomeration effects are concerned. The improvements in order to facilitate agglomeration as described in the methodology section are demonstrated later in the study.

Since the stochastic technique had up to this point been consistent with the deterministic as far as the collision rate was concerned, this effect was of interest. It was initially theorized to be because of an underestimation in the collision energy, or some other peculiarity of the stochastic technique. Even a small change in collision rate would quickly accumulate to a large change in the effects of agglomeration, and the stochastic technique did exhibit an increased collision rate compared to the deterministic approach. This increase was further determined to be a small part of the effect. What was quickly ascertained was that the collision rate dropped substantially when agglomeration was implemented for the deterministic simulation of particles, with Tab.1 showing the scale of this decrease to be of at least an order of magnitude.

Investigating the cause of the change in collision rate was carried out through analysis of the collision location within the channel. The locations of collisions taking place over the course of 100 simulation time steps were recorded and are illustrated in Fig.2. For the purpose of easier visualization, a sector of the channel was chosen that is one half of the total length, width, and breadth of the entire geometry.

Each individual point in the figure represents the location of a collision between two particles. These positions tend to form dotted lines, particularly towards the center of the channel. These would appear to indicate multiple collisions occurring in the same relative places over the course of the simulation. The fact that these lines follow fluid streamlines is indicative of this, and indeed what is being observed here is particles that are confined to the same fluid eddies colliding with each other repeatedly.

**Table 1.** Comparisons of deterministic collision rates per bulk time unit for cases with and without agglomeration.

Case	300k, $r_p^* = 0.005$	2.2M, $r_p^* = 0.005$	300k, $r_p^* = 0.01$
Collisions without agglomeration	2218	160 847	10 447
Collisions with agglomeration	214	10 299	1707

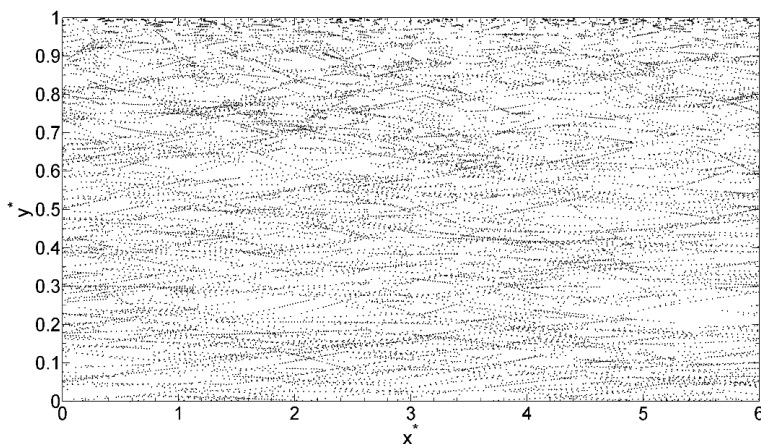


**Figure 2.** Visualisation of the location (plotted as dots) of deterministic collisions in the  $x^*-y^*$  plane for a section of a channel flow in which the 300k, 100  $\mu\text{m}$  ( $r_p^* = 0.005$ ) particle case is being simulated with four-way coupling, over 100 time steps.

A numerical analysis of this effect was performed, shown in Fig. 3. For this, data on a selection of collisions from the deterministic simulations without agglomeration were collected for the three different cases considered over a hundred time steps. The total number of collisions was compared to the number of repeat collisions between particles, i.e., the total number minus the number of collisions between two particles that had not collided thus far in the simulation.

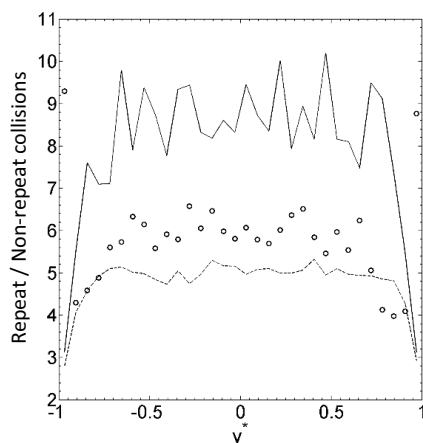


**Figure 3.** Proportion of deterministic collisions taking place across the channel which reoccur for the three particle cases simulated in this study. —  $N_p = 300k$ , 100  $\text{m}$  ( $r_p^* = 0.005$ ); ---  $N_p = 2.2M$ , 100  $\text{m}$  ( $r_p^* = 0.005$ ); ○  $N_p = 300k$ , 200  $\text{m}$  ( $r_p^* = 0.01$ ).

Comparing the repeat collisions across the channel to the total number within that section indicated that most repeat collisions (see Fig. 3) take place at the center of the channel, where the flow is least turbulent. The simulation with the lowest radius and particle number had the lowest collision rate overall, and this makes it something of an outlier, with repeat collisions being far more likely to occur than for any two given particles to encounter each other for the first time.

The  $r_p^* = 0.01$  case also has some unique properties, with an increase in repeat collisions in the wall regions. This is caused by turbophoresis moving high-speed particles to those regions. Overall, increasing either the number or size of particles produces a higher collision rate. This also has the effect of increasing the proportion of non-repeat or first time collisions from particles that are not as constrained by eddies or are travelling between them through effects like turbophoresis. The collision rate is still dominated by particles that are kept in proximity by localized fluid effects.

These conditions, due to continuous proximity and repeated chances for collision, cause a greater frequency of particle collision when this is considered as a factor in the simulation. Where agglomeration is involved, particles in similar local fluid regions agglomerate quickly, and their effect on the collision rate rapidly becomes negligible, although this effect is likely to be dependent on the coefficient of restitution. As a result, the collision rate drops quickly and stabilizes at a much lower value than predicted by the four-way coupled simulation without agglomeration. This can be seen in Fig. 4, which shows the collision rate over time.

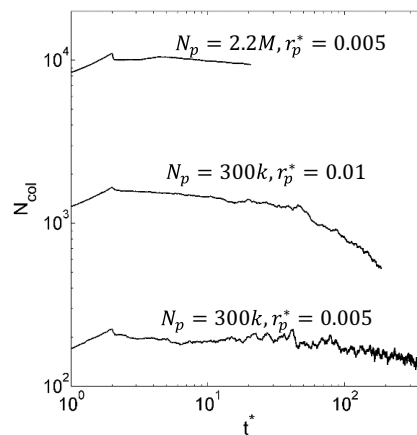


**Figure 4.** Temporal evolution of number of collisions per time step for the three deterministic cases colliding with agglomeration.

Here, each plot indicates an initial spike of collisions. This is an artifact of the initial conditions, which took particle statistics from an already settled flow without agglomeration. This illustrates an effect larger than the reduction in collision rate over time as more and more particles agglomerate. The case with the large radius particles is the only one where the collision rate changes comparably. The collision step of the high concentration case was long, the very reason for developing the stochastic technique in the first place, so simulations for that case were performed for shorter times.

The stochastic simulation of the four-way coupled system, however, considers only the advective forces on the particles, and their sizes in the calculation of collision rate. This does not quickly change with the implementation of agglomeration, and

as a result the collision rate remains a close match to the first set of values in Tab. 1, rather than the correct second set. This in turn results in a high agglomeration rate that swiftly leads to very large particles.

Wang et al. [15] described impacts known as the accumulation effect and the turbulent transport effect. These were potential candidates for the cause of the repeat collision effect that has been observed in this study, so calculations for the magnitude of these effects were implemented into the formulas the stochastic technique uses for the collision rate. This had the desired effect of reducing the rate of collision, and therefore agglomeration, but as Tab. 2 and Fig. 5 demonstrate, this reduction was not equal to the size of the effect.

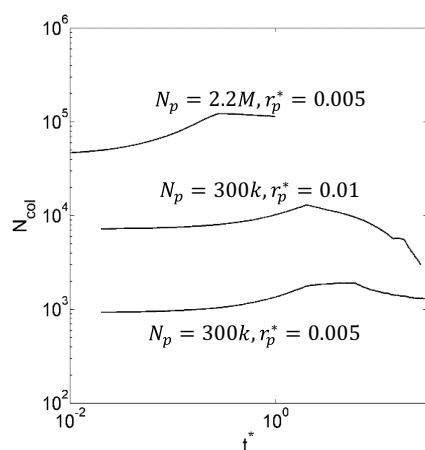


**Figure 5.** Temporal evolution of number of collisions per time step for the three stochastic cases colliding with agglomeration.

Fig. 5 displays the collision rate over time for the stochastic agglomeration technique. For the higher concentration case the agglomeration rate was still significant enough that the time step had to be reduced by orders of magnitude, to  $10^{-4}$ , for the simulation to not diverge due to high-Stokes number particle interaction with the fluid. This is why the logarithmic time axis starts earlier for the high concentration case.

In Fig. 6 the sizes of different aggregates formed over time have been plotted for both the deterministic and stochastic methods. Here, it can be seen that even with the improvements, the collision rate, and therefore the agglomeration rate, is being overpredicted with, e.g., the size 40 agglomerates for the  $r_p^* = 0.01$  case occurring at around  $t^* = 10$ , rather than  $t^* = 150$  as occurred for the corresponding deterministic case.

**Table 2.** Comparisons of deterministic and stochastic runtimes and collision rates for cases with and without agglomeration.

Case	300k, $r_p^* = 0.005$	2.2M, $r_p^* = 0.005$	300k, $r_p^* = 0.01$
Deterministic runtime	2.43	17.75	3.09
Deterministic collisions/ $t^*$	214	10 299	1707
Stochastic runtime	2.19	13.41	2.53
Stochastic collisions/ $t^*$	1895	72 862	15 291

Figs. 7 and 8 plot the mean streamwise velocities and stresses, and particle concentrations, across the channel, respectively. These results show the consequences of the overpredictions of aggregation rate. For the cases with smaller particles, the concentration plots demonstrate a relatively small overall change. The agglomeration rate in this case still results in a great proportion of single particles over time, whichever agglomeration technique is used, meaning that the multiphase flow properties are resilient. This is backed up by the results in Fig. 8 where said cases show minimal differences, a consistent property of the  $r_p^* = 0.005$  particles for this study. The higher concentration of these particles actually has a slowing effect on the fluid near the bulk of the flow, as indicated in Fig. 7, as energy is transferred from the fluid phase to speed up new particles with higher inertia.

The  $r_p^* = 0.01$  particles show a predictable rise in the streamwise normal stresses, where the increased Stokes number of the particle phase, overall, decouples them from the fluid phase, in this case at a faster rate than a comparable deterministic simulation. This case also has a surprising spike in particle concentration near to the center of the flow (Fig. 8b). While all the stochastic agglomeration cases show similar distributions, with peaks at the wall and in the flow bulk region, this case is particular in having a decrease at the very center of the flow, where extremely large agglomerates have begun to move to the wall through turbophoresis.

The changes in particle concentration across the channel for the  $r_p^* = 0.005$  particles is similar between the deterministic and stochastic techniques, differing only in magnitude. This suggests that overprediction of agglomeration is temporal in nature, and that similar distributions of particle sizes will behave the same irrespective of the time steps needed to reach that state.

## 4 Conclusions

The impact of stochastic particle agglomeration on previously studied four-way coupled particle-laden channel flows has been investigated, with a focus on a repeat collision effect which causes inaccuracies in the agglomeration rate. With agglomeration implemented, the simulation of particle-laden channel flows gains versatility and accuracy for more complex multiphase flows, in that aggregation, which encourages particle deposition which can lead to flow blockages, can be captured. For this particular geometry and the particles Stokes numbers considered, the effect of the particles on the fluid flow was small, with the most significant effects found for the higher Stokes number particle case.

While applying the agglomeration mechanism to a previously successful stochastic DSMC technique, an inconsistency emerged which led to an investigation into what is termed the repeat collision effect. This effect turned out to be a direct result of fluid streamlines in the bulk flow confining low Stokes

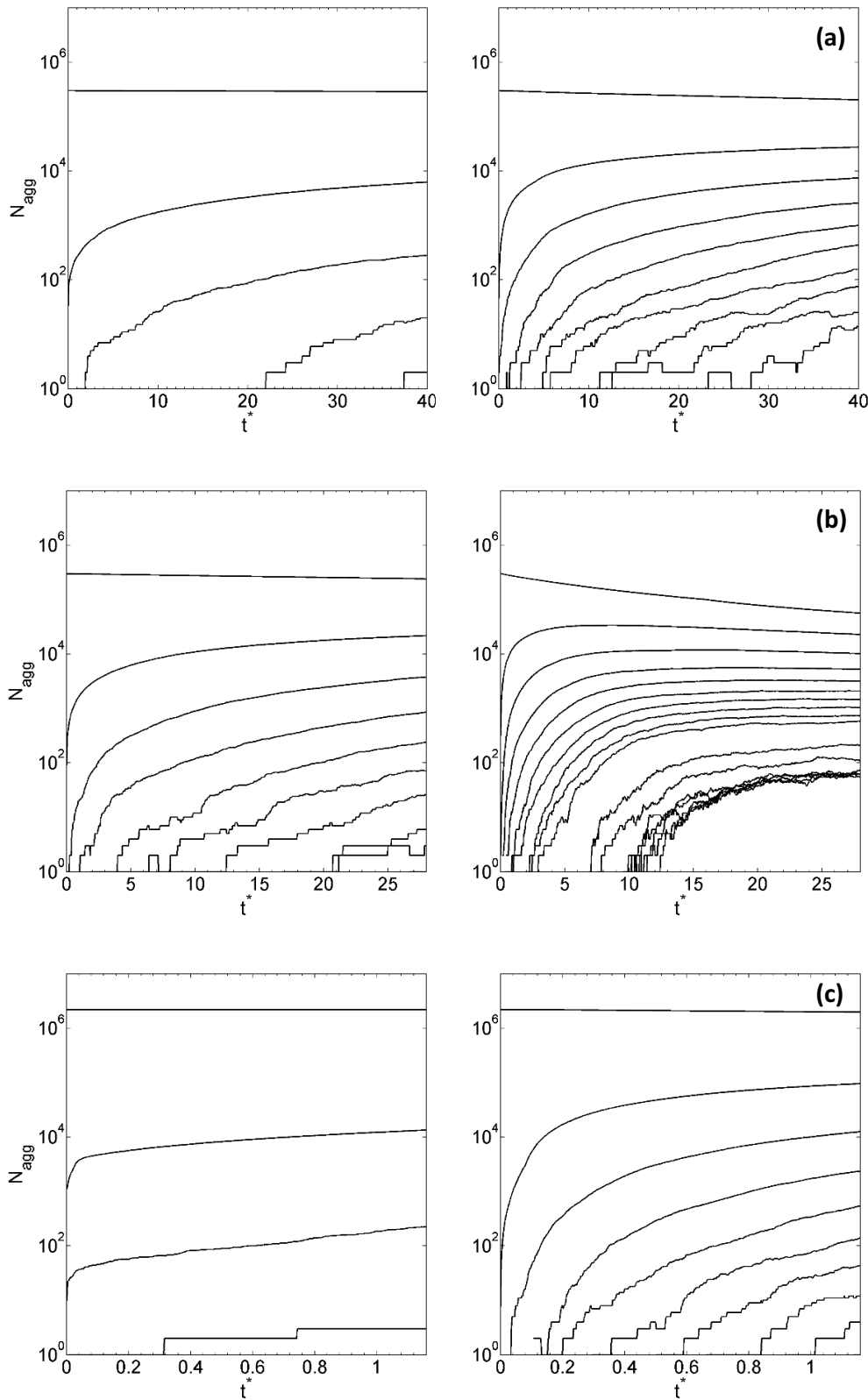


**Figure 6.** Number of differently sized agglomerates  $N_{agg}$  over time for agglomeration using deterministic (left) and stochastic (right) techniques for particles with sizes 1, 2, 3 ... 9 and 10, 15, ... 50 (top to bottom). For simulations with (a) 300k, 100  $\mu\text{m}$  ( $r_p^* = 0.005$ ), (b) 300k, 200  $\mu\text{m}$  ( $r_p^* = 0.01$ ), and (c) 2.2M, 100  $\mu\text{m}$  particles.

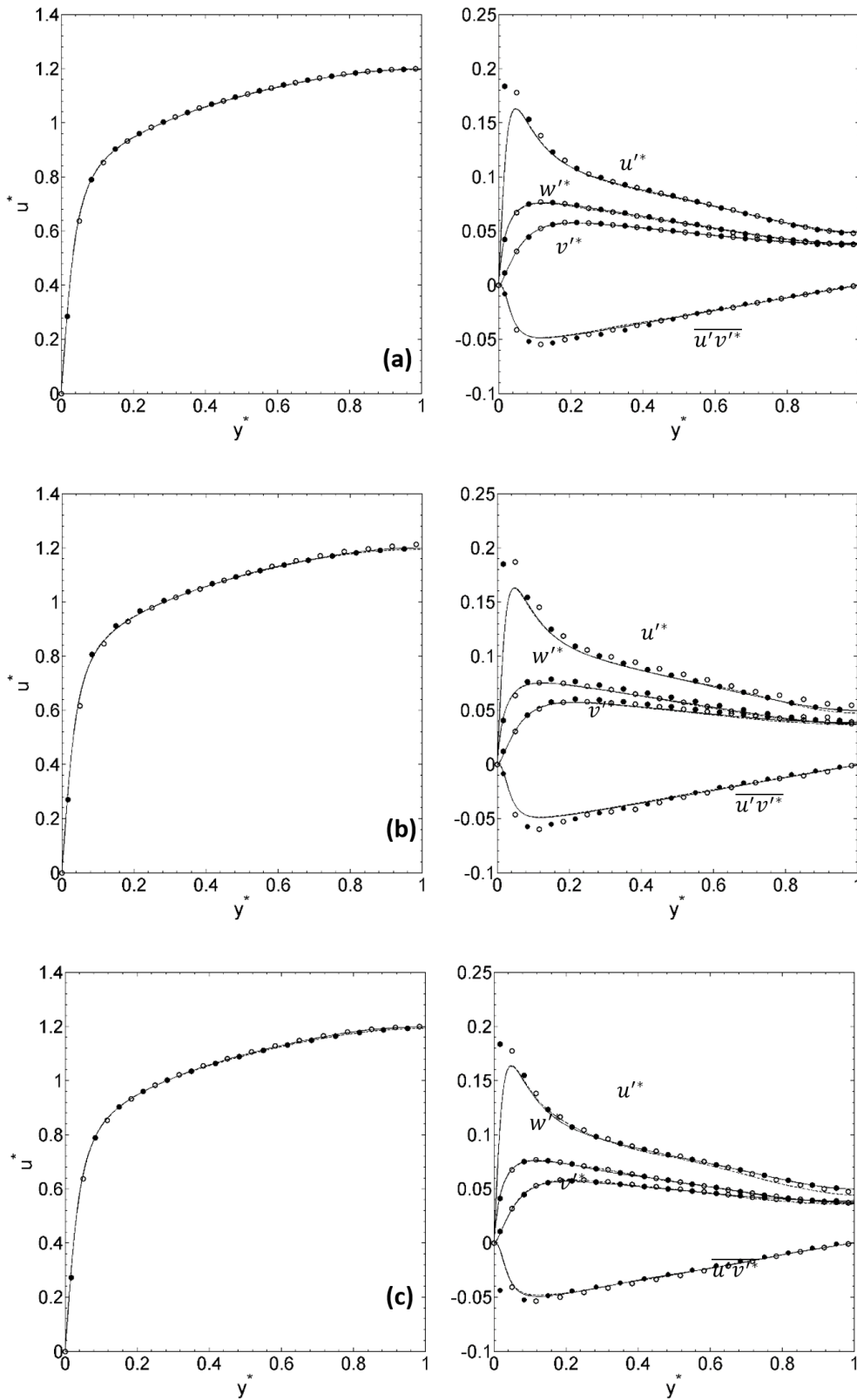


**Figure 7.** Mean streamwise velocities  $u^*$  and normal and shear stresses  $u'^*$ ,  $v'^*$ ,  $w'^*$ ,  $u'v'^*$  for fluid flows with particles collided using deterministic and stochastic inter-particle collision techniques with agglomeration. Fluid simulated using — deterministic and - - - stochastic technique, and particles with ● deterministic and ○ stochastic collisions with agglomeration. For simulations with (a) 300k, 100  $\mu\text{m}$  ( $r_p^* = 0.0005$ ), (b) 300k, 200  $\mu\text{m}$  ( $r_p^* = 0.01$ ), and (c) 2.2M, 100  $\mu\text{m}$  particles.

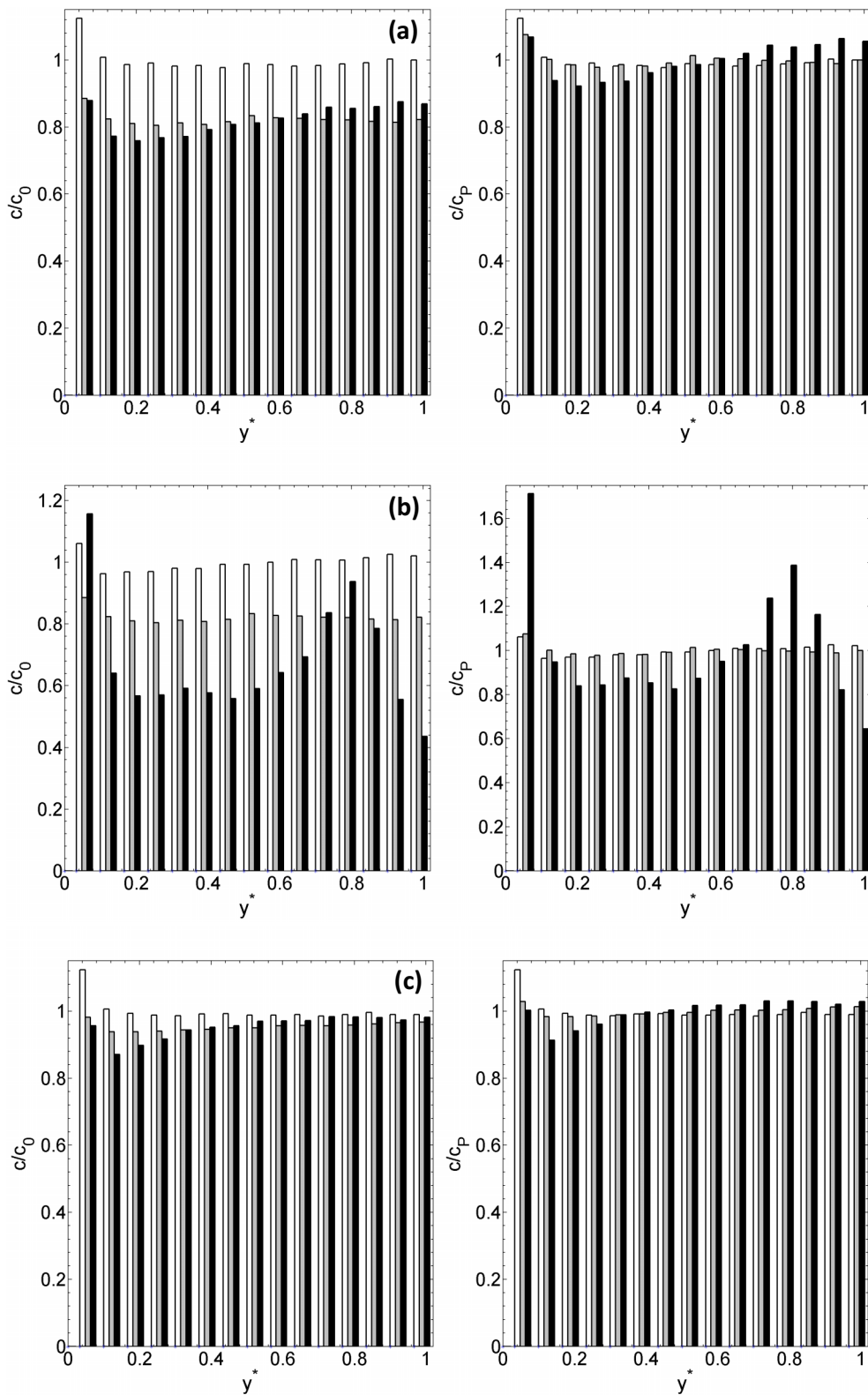


**Figure 8.** Particle concentration ( $c/c_0$ ), and concentration ( $c/c_p$ ) relative to total number of particles, across the channel for four-way coupled flows with no agglomeration (white bars), deterministic agglomeration (gray bars), and stochastic agglomeration (black bars). For simulations with (a) 300k, 100  $\mu\text{m}$  ( $r_p^* = 0.005$ ), (b) 300k, 200  $\mu\text{m}$  ( $r_p^* = 0.01$ ), and (c) 2.2M, 100  $\mu\text{m}$  particles.

number particles to close proximity, which would then collide repeatedly, skewing the number of reported collisions. The stochastic technique, previously observed to match this reported number of collisions, did not account for the agglomeration of the confined particles, leaving isolated agglomerates with a magnitude lower collision rate. It therefore agglomerated particles at an inordinate rate with a devastating effect on the accuracy of the simulations.

An attempt was made to rectify this through modifications based on a study of particle accumulation and turbulent transport effects, and this had some success, reducing the collision and agglomeration rates, though not enough to make the simulation accurate when compared to a deterministic approach. As improvements to the stochastic technique for handling inter-particle collisions are ongoing, it is expected that further work on this technique will lead to a more effective solution to the repeat collision effect. In the meantime, the stochastic technique has proven an effective way to reduce computational cost in cases where its inconsistencies with the deterministic approach are acceptable.

In the current work the coefficient of restitution was set to a consistent value, matching collisions between calcite particles in a water flow. The results made it clear that the chance of agglomeration directly has an impact on the repeat collision effect. Further work also needs to consider this relationship. The agglomeration probability could be increased by lowering the coefficient of restitution, and this is expected to be the cause of the most significant deviations between collision rates with and without agglomeration.

## Acknowledgment

D. R. would like to thank the Engineering and Physical Sciences Research Council in the UK, and the National Nuclear Laboratory, who funded the work described as part of the EPSRC Centre for Doctoral Training in Nuclear Fission – Next Generation Nuclear.

*The authors have declared no conflict of interest.*

## Symbols used

$C_D$	[-]	drag coefficient
$C_L$	[-]	lift coefficient
$d_p^*$	[-]	particle diameter
$e_n^2$	[-]	coefficient of restitution
$\mathbf{f}_i$	[-]	body forces on cell $i$
$f_{PG}$	[-]	pressure gradient force
$\mathbf{f}_{2W}^i$	[-]	two-way coupling force
$H^*$	[-]	Hamaker constant
$M_{VM}$	[-]	virtual or added mass term
$p^*$	[-]	pressure
$P_{coll}$	[-]	collision probability
$r_p^*$	[-]	particle radius
$Re_B$	[-]	bulk Reynolds number
$Re_\tau$	[-]	shear Reynolds number
$t^*$	[-]	time

$u_\eta$	[-]	Kolmogorov velocity scale
$\mathbf{u}^*$	[-]	fluid velocity vector
$U_B$	[m s <sup>-1</sup> ]	fluid bulk velocity
$u_F^*$	[-]	fluid velocity
$u_s^*$	[-]	slip velocity
$V_i^*$	[-]	volume of a computational cell
$\mathbf{x}_P^*$	[-]	particle position

## Greek letters

$\delta$	[m]	channel half-height
$\delta_0^*$	[-]	minimum contact distance
$\varepsilon$	[m <sup>2</sup> s <sup>-2</sup> ]	turbulence energy dissipation rate
$\eta$	[-]	Kolmogorov length scale
$\nu$	[m <sup>2</sup> s <sup>-1</sup> ]	kinematic viscosity
$\rho_F$	[kg m <sup>-3</sup> ]	fluid phase density
$\rho_P$	[kg m <sup>-3</sup> ]	particle phase density
$\boldsymbol{\tau}^*$	[-]	deviatoric stress tensor
$\omega_F^*$	[-]	fluid vorticity

## Sub- and superscripts

$x, y, z$	Cartesian coordinates
*	non-dimensional units

## Abbreviations

DNS	direct numerical simulation
DSMC	direct simulation Monte Carlo
LES	large eddy simulation
LPT	Lagrangian particle tracking
SEM	spectral element method

## References

- [1] I.-B. Lee, J. P. P. Bitog, S.-W. Hong, I.-H. Seo, K.-S. Kwon, T. Bartzanas, M. Kacira, *Comput. Electron. Agric.* **2013**, *93*, 168–183. DOI: <https://doi.org/10.1016/j.compag.2012.09.006>
- [2] A. Chakravarti, N. A. Patankar, M. V. Panchagnula, *Phys. Fluids* **2019**, *31* (12), 121901. DOI: <https://doi.org/10.1063/1.5127787>
- [3] D. Guha, P. A. Ramachandran, M. P. Dudukovic, *Chem. Eng. Sci.* **2007**, *62* (22), 6143–6154. DOI: <https://doi.org/10.1016/j.ces.2007.06.033>
- [4] L. Raynal, F. Augier, F. Bazer-Bachi, Y. Haroun, C. Pereira da Fonte, *Oil Gas Sci. Technol.* **2016**, *71* (3), 42. DOI: <https://doi.org/10.2516/ogst/2015019>
- [5] C. Marchioli, A. Soldati, *J. Fluid Mech.* **2002**, *468*, 283–315. DOI: <https://doi.org/10.1017/S0022112002001738>
- [6] Y. Li, J. B. McLaughlin, K. Kontomaris, L. Portela, *Phys. Fluids* **2001**, *13* (10), 2957–2967. DOI: <https://doi.org/10.1063/1.1396846>
- [7] M. Sommerfeld, *Int. J. Multiphase Flow* **2001**, *27* (10), 1829–1858. DOI: [https://doi.org/10.1016/S0301-9322\(01\)00035-0](https://doi.org/10.1016/S0301-9322(01)00035-0)
- [8] P. F. Fischer, J. W. Lottes, S. G. Kerkemeier, *Nek5000*, **2008**. <http://nek5000.mcs.anl.gov>
- [9] R. D. Moser, P. Moin, *NASA Technical Memorandum 85974*, **1984**.
- [10] *An Introduction to Numerical Analysis* (Eds: E. Süli, D. Meyers), Cambridge University Press, Cambridge **2003**.

- [11] D. O. Njobuenwu, M. Fairweather, *Phys. Fluids* **2017**, *29* (8), 083301. DOI: <https://doi.org/10.1063/1.4997089>
- [12] D. A. Rupp, L. F. Mortimer, M. Fairweather, in *Proc. 13th Int. ERCOFTAC Symp. on Engineering, Turbulence, Modelling and Measurements*, **2021**.
- [13] P. G. Saffman, S. J. Turner, *J. Fluid Mech.* **1956**, *1* (1), 16–30. DOI: <https://doi.org/10.1017/S0022112056000020>
- [14] S. K. Pawar, J. T. Padding, N. G. Deen, A. Jongsma, F. In-nings, J. A. M. Kuipers, *Chem. Eng. Sci.* **2014**, *105*, 132–142. DOI: <https://doi.org/10.1016/j.ces.2013.11.004>
- [15] L. P. Wang, A. S. Wexler, Y. Zhou, *J. Fluid Mech.* **2000**, *415*, 117–153. DOI: <https://doi.org/10.1017/S0022112000008661>
- [16] D. A. Rupp, D. O. Njobuenwu, M. Fairweather, in *Proc. 12<sup>th</sup> Int. ERCOFTAC Symp. on Engineering, Turbulence, Modelling and Measurements*, **2018**.